International Journal of Solids and Structures 50 (2013) 30–37

Contents lists available at SciVerse ScienceDirect

International Journal of Solids and Structures

journal homepage: www.elsevier.com/locate/ijsolstr

Exact buckling loads of two-layer composite Reissner's columns with interlayer slip and uplift

S. Schnabl *, I. Planinc

University of Ljubljana, Faculty of Civil and Geodetic Engineering, Jamova 2, SI-1115 Ljubljana, Slovenia

ARTICLE INFO

Article history:
Received 3 February 2012
Received in revised form 28 August 2012
Available online 10 September 2012

Keywords:
Buckling
Layers
Uplift
Slip
Exact

ABSTRACT

The principal purpose of the paper is to present an efficient mathematical model for studying the buckling behaviour of geometrically perfect, elastic Reissner's two-layer composite columns with interlayer slip and uplift between the layers. The present mathematical model is capable of predicting exact critical buckling loads and corresponding buckling modes. Thus, it is used to study the influence of the transverse interlayer stiffness in combination with the longitudinal interlayer stiffness on critical buckling loads and modes. This effect is proved to be significant. The critical buckling loads calculated by the proposed method can be up to approximately 89% smaller than those where interlayer uplift is neglected.

1. Introduction

Layered composite structures are of practical importance in many engineering applications, especially in civil engineering. The reason for their wide-spread application is that they have numerous advantages over the conventional structures, such as a high strength-to-weight ratio, a high stiffness-to-weight ratio, and many more. In spite of their many attractive qualities, layered composites do, however, often suffer from partial interaction between the layers. As a result, interlayer slip and uplift between the layers develop which can, in some cases, significantly affect the mechanical behaviour of the layered composite system.

A large number of references exist in the literature on modelling of incomplete interaction between the layers. A majority of the papers only dealt with the analysis of interlayer slip between the layers while uplift is ignored. For bending problems see e.g. (Erkmen and Attard, 2011; Girhammar and Pan, 2007; Kim and Choi, 2011; Nguyen et al., 2011a,b; Ranzi et al., 2010; Schnabl et al., 2007), while for buckling problems see e.g. (Amadio and Bedon, 2011; Challamel and Girhammar, 2011, 2012; Chen and Qiao, 2011; Grognec et al., 2012; Kryžanowski et al., 2009; Schnabl and Planinc, 2010, 2011).

Much less literature is available on the modelling of a combined effect of interlayer slip and uplift on the mechanical behaviour of layered composite structures. The analytical models taking both slip and uplift into account have been proposed by Adekola (1968), Kroflič et al. (2010a), Nguyen et al. (2001) and Robinson and Naraine (1988). Besides, some numerical formulations have been proposed that take into account a bi-linear or a fully non-linear interface law (Gara et al., 2006; Kroflič et al., 2010b; Ranzi et al., 2005, 2006). Only very recently, a new finite element formulation for a fully geometrically and materially non-linear analysis of bending of two-layer beams with both interlayer slip and uplift has been presented by Kroflič et al. (2011).

However, as far as the author's knowledge is concerned it seems that there exists no formulation in the open literature for a buckling analysis of two-layer composite Reissner's columns with interlayer slip and uplift between the layers. Consequently, the aim of the present papers is to derive an exact mathematical model for the aforementioned buckling analysis of two-layer composite columns. For this purpose, a model previously presented by Schnabl and Planinc (2011) has been upgraded to the model that takes into account also the interlayer uplift.

In the numerical examples, the critical buckling loads and modes are calculated for a wide range of possible material and geometric parameters, such as interlayer slip modulus, K, interlayer uplift modulus, C, and different boundary conditions. Thus, the effect of the interlayer uplift on the critical buckling loads and modes is investigated in detail.

2. Theory

Consider a geometrically perfect, initially straight, planar, two-layer composite column as shown in Fig. 1. The column has an undeformed length L. In general, it is made from two dissimilar

* Corresponding author. Tel.: +386 31 389425.
E-mail addresses: simon.schnabl@fgg.uni-lj.si, sschnabl@fgg.uni-lj.si, katja.schnabl@guest.arnes.si (S. Schnabl).

0020-7683/$ - see front matter
http://dx.doi.org/10.1016/j.ijsolstr.2012.08.027

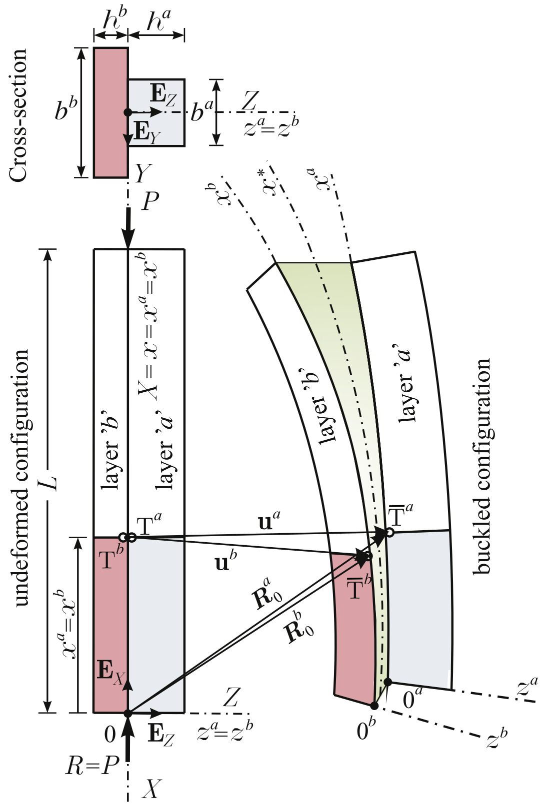

Fig. 1. Two-layer composite column. Initial undeformed and current buckled configurations.

layers, a and b, joined by a layer of negligible thickness and finite stiffness in normal and tangential directions. Each layer is modelled by Reissner's large-displacement finite-strain shear-deformable beam theory (Reissner, 1972). The column is placed in a (X,Z) plane of spatial Cartesian coordinate system with coordinates (X,Y,Z) and unit base vectors $\mathbf{E}_X$, $\mathbf{E}_Y$ and $\mathbf{E}_Z = \mathbf{E}_X \times \mathbf{E}_Y$. The initial undeformed reference axis of the layered column is common to both layers. It is parametrized by the undeformed arc-length x. Material particles of each layer are identified by material coordinates x^i, y^i, z^i $(i = a, b)$ in local coordinate system which are assumed to coincide initially with spatial coordinates, and then follow the deformation of the column. Thus, $x^a \equiv x^b \equiv x \equiv X$, $y^a \equiv y^b \equiv y \equiv Y$, and $z^a \equiv z^b \equiv z \equiv Z$ in the initial undeformed configuration. The column is loaded axially through its ends by a conservative compressive force, P. For further details an interested reader is referred to Schnabl and Planinc (2010, 2011)).

2.1. Governing equations

The system of governing equations of the two-layer composite column consists of kinematic, equilibrium, and constitutive equations along with the boundary conditions for each of the layers. In addition, each individual layer is assembled into a two-layer composite column by the constraining equations. While the governing equations of the individual layer have been already described in detail by Schnabl and Planinc (2011) and Kroflič et al. (2011), only new constraining equations and a final linearized form of the whole system of the governing equations will be described next. In what follows, superscripts a and b indicate that quantities are related to layers a and b, respectively.

2.1.1. Constraining equations

The layer a of the two-layer composite column under deformation is constrained to follow the deformation of the layer b, and vice versa. It has been shown by Wells et al. (2002) and Kroflič et al. (2011) that it is suitable to express the constraining equations in the so-called "mean" contact axis x^* with normal and tangential base vectors, $\boldsymbol{e}_t^*$ and $\boldsymbol{e}_n^*$, as (see Fig. 2):

$$\boldsymbol{e}_t^* = \frac{\zeta \boldsymbol{e}_t^a + (1-\zeta)\boldsymbol{e}_t^b}{\|\zeta \boldsymbol{e}_t^a + (1-\zeta)\boldsymbol{e}_t^b\|_2} = e_{tX}^* \mathbf{E}_X + e_{tZ}^* \mathbf{E}_Z, \tag{1}$$

$$\boldsymbol{e}_n^* = \frac{\zeta \boldsymbol{e}_n^a + (1-\zeta)\boldsymbol{e}_n^b}{\|\zeta \boldsymbol{e}_n^a + (1-\zeta)\boldsymbol{e}_n^b\|_2} = e_{nX}^* \mathbf{E}_X + e_{nZ}^* \mathbf{E}_Z, \tag{2}$$

where $\boldsymbol{e}_t^i$ and $\boldsymbol{e}_n^i$ $(i = a, b)$ represent the deformed tangential and normal base vectors in the contact point of layers a and b, ζ represents the weight with a value between 0 and 1, $\| \bullet \|_2$ is the Euclidean vector norm, and $e_{tX}^*, e_{tZ}^*, e_{nX}^*, e_{nZ}^*$ denote the components of the unit base vectors $\boldsymbol{e}_t^*$ and $\boldsymbol{e}_n^*$ in the spatial Cartesian coordinate system.

A stress-constraint requirement is determined from the third Newton's law, which ensures an equilibrium of the interlayer contact tractions of the particles in contact. This requirement is expressed in the vector-valued function form as

$$\mathrm{d}\boldsymbol{F}^a + \mathrm{d}\boldsymbol{F}^b = \mathbf{0} \rightarrow \boldsymbol{p}^a \mathrm{d}x^a + \boldsymbol{p}^b \mathrm{d}x^b = \mathbf{0} \xrightarrow{\mathrm{d}x^a = \mathrm{d}x^b} \boldsymbol{p}^a + \boldsymbol{p}^b = \mathbf{0}, \tag{3}$$

where $\boldsymbol{p}^a$ and $\boldsymbol{p}^b$ are the interlayer contact tractions, measured per unit of layer's undeformed length. Hence, from Eq. (3)

$$\boldsymbol{p} = \boldsymbol{p}^a = -\boldsymbol{p}^b = p_X \mathbf{E}_X + p_Z \mathbf{E}_Z. \tag{4}$$

When written along the $\boldsymbol{e}_t^*$ and $\boldsymbol{e}_n^*$, the components p_X and p_Z can be expressed with respect to the mean basis as

$$p_X = p_t^* e_{tX}^* + p_n^* e_{nX}^*, \tag{5}$$

$$p_Z = p_t^* e_{tZ}^* + p_n^* e_{nZ}^*, \tag{6}$$

where p_t^* and p_n^* are the components of the contact tractions along the mean basis.

In order to define a general constitutive law of the contact, it is again convenient to describe the components of the displacements vectors $\boldsymbol{u}^i$ with respect to the mean base $(\boldsymbol{e}_t^*, \boldsymbol{e}_n^*)$ as:

$$u_t^{i*} = \boldsymbol{u}^i \cdot \boldsymbol{e}_t^*, \tag{7}$$

$$w_n^{i*} = \boldsymbol{u}^i \cdot \boldsymbol{e}_n^*. \tag{8}$$

A mean interlayer slip, Δ^*, and a mean interlayer uplift, d^*, are thus defined as

$$\Delta^* = u_t^{a*} - u_t^{b*}, \tag{9}$$

$$d^* = w_n^{a*} - w_n^{b*}. \tag{10}$$

In general, a cohesive constitutive law of the contact considers a mixed mode delamination with simultaneous sliding and uplifting.

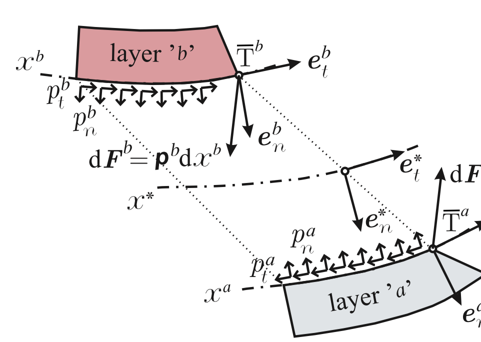

Fig. 2. Geometrical meaning of the mean contact line. Base vectors and contact tractions.

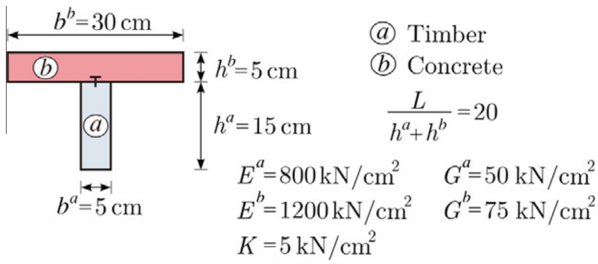

Fig. 3. Geometrical and material properties of a timber-concrete column.

Table 1
Two-layer composite column boundary conditions.

Classical cases	C–F	C–C	C–P	P–P
Non-zero values s_i	$s_2^0 = s_4^0 = 1$	$s_2^0 = s_4^0 = 1$	$s_2^0 = s_4^0 = 1$	$s_2^0 = s_4^0 = 1$
	$s_6^0 = s_8^0 = 1$	$s_6^0 = s_8^0 = 1$	$s_6^0 = s_8^0 = 1$	$s_6^0 = s_8^0 = 1$
	$s_{10}^0 = s_{12}^0 = 1$	$s_{10}^0 = s_{12}^0 = 1$	$s_{10}^0 = s_{12}^0 = 1$	$s_9^0 = s_{11}^0 = 1$
	$s_1^L = s_3^L = 1$	$s_1^L = s_3^L = 1$	$s_1^L = s_3^L = 1$	$s_1^L = s_3^L = 1$
	$s_5^L = s_7^L = 1$	$s_6^L = s_8^L = 1$	$s_6^L = s_8^L = 1$	$s_6^L = s_8^L = 1$
	$s_9^L = s_{11}^L = 1$	$s_{10}^L = s_{12}^L = 1$	$s_9^L = s_{11}^L = 1$	$s_9^L = s_{11}^L = 1$

C = clamped (fixed); F = free; P = pinned.

The contact tractions, however, are mutually dependent on Δ^* and d^* (see, e.g. (Volokh et al., 2002; Alfano and Crisfield, 2001))

$$p_t^* = \mathcal{K}(d^*, \Delta^*), \tag{11}$$

$$p_n^* = \mathcal{C}(d^*, \Delta^*). \tag{12}$$

Since in most civil engineering applications, a cohesive interface law can be decoupled in each direction, Eqs. (13), (14) can be approximated as (Gara et al., 2006; Ranzi et al., 2006)

$$p_t^* = \mathcal{K}(\Delta^*), \tag{13}$$

$$p_n^* = \mathcal{C}(d^*). \tag{14}$$

In the literature, bi-linear interface laws are often considered, e.g. a bi-linear interface law for slip (Foraboschi, 2009), and bi-linear or fully non-linear interface law for uplift (Alfano and Crisfield, 2001; Gara et al., 2006; Kroflič et al., 2011; Ranzi et al., 2006). In the present paper, only linear interface laws for slip and uplift will be considered.

2.1.2. Linearized stability equations

To obtain the general linearized stability equations for a determination of critical loads, a linearized stability theory is applied. This theory is based on the supposition that critical loads of the non-linear system and corresponding linearized system coincide (Keller, 1970). In order to apply the linearized equations to a two-layer composite column buckling, the equations proposed by Kroflič et al. (2011) have to be evaluated in the primary configuration which is in this case any arbitrary deformed configuration in which the two-layer composite column remains straight without interlayer slip and uplift. The notation is explained in detail by Schnabl and Planinc (2011) and Kroflič et al. (2011). Finally, the linear buckling equations of the two-layer composite column are defined as:

Kinematic equations:

$$\begin{aligned}
\delta u^{a\prime} &= \delta\varepsilon^a,\\
\delta u^{b\prime} &= \delta\varepsilon^b,\\
\delta w^{a\prime} &= -(1+\varepsilon)\delta\varphi^a + \delta\gamma^a,\\
\delta w^{b\prime} &= -(1+\varepsilon)\delta\varphi^b + \delta\gamma^b,\\
\delta\varphi^{a\prime} &= \delta\kappa^a,\\
\delta\varphi^{b\prime} &= \delta\kappa^b,
\end{aligned} \tag{15}$$

Equilibrium equations:

$$\begin{aligned}
\delta R_X^{a\prime} &= \delta\mathcal{N}^{a\prime} = \delta p_t,\\
\delta R_X^{b\prime} &= \delta\mathcal{N}^{b\prime} = -\delta p_t,\\
\delta R_Z^{a\prime} &= \delta p_n,\\
\delta R_Z^{b\prime} &= -\delta p_n,\\
\delta M_Y^{a\prime} &= -\mathcal{N}^a \delta w^{a\prime} + (1+\varepsilon)\delta R_Z^a - \delta m_Y^a = 0,\\
\delta M_Y^{b\prime} &= -\mathcal{N}^b \delta w^{b\prime} + (1+\varepsilon)\delta R_Z^b - \delta m_Y^b = 0,
\end{aligned} \tag{16}$$

Constitutive equations:

$$\begin{aligned}
\delta R_X^a &= \delta\mathcal{N}^a = C_{11}^a \delta\varepsilon^a + C_{12}^a \delta\kappa^a,\\
\delta R_X^b &= \delta\mathcal{N}^b = C_{11}^b \delta\varepsilon^b + C_{12}^b \delta\kappa^b,\\
\delta R_Z^a &= -R_X^a \delta\varphi^a + C_{33}^a \delta\gamma^a,\\
\delta R_Z^b &= -R_X^b \delta\varphi^b + C_{33}^b \delta\gamma^b,\\
\delta M_Y^a &= C_{21}^a \delta\varepsilon^a + C_{22}^a \delta\kappa^a,\\
\delta M_Y^b &= C_{21}^b \delta\varepsilon^b + C_{22}^b \delta\kappa^b,
\end{aligned} \tag{17}$$

Table 2
The critical buckling loads of P–P two-layer composite column for various *K*s and *C*s.

C^a / K^a	10^{-3}	10^{-2}	10^{-1}	1	10	10^2	∞^b
P_{cr}[kN]							
10^{-10}	47.534513	80.074021	89.765236	90.881674	90.994878	91.006214	91.007473
10^{-5}	47.535188	80.076243	89.768059	90.884568	90.997780	91.009116	91.010376
10^{-3}	47.601669	80.295598	90.046852	91.170397	91.284322	91.295731	91.296999
10^{-2}	48.180007	82.232032	92.517928	93.704983	93.825370	93.837425	93.838765
10^{-1}	52.202794	97.257194	102.17982	114.12040	114.30166	114.31976	114.32178
1	60.994209	144.55766	184.54079	189.75778	190.30141	190.35458	190.36076
10^1	66.367806	197.25893	286.92709	299.08284	300.33612	300.45772	300.47186
10^2	67.559568	212.62507	323.65468	339.28525	340.87918	341.00389	341.04721
10^3	67.704022	214.56415	328.76655	344.85020	346.49739	346.63609	346.66198
10^5	67.720133	214.78185	329.36609	345.48453	347.13784	347.30326	347.32169
10^{10}	67.720296	214.78405	329.37219	345.49096	347.14433	347.31005	347.32847

[a] In [kN/cm^2].
[b] P_{cr} calculated by Schnabl and Planinc (2011), where $d = 0$.

Table 3
The critical buckling loads of P–P two-layer composite column for various Ks and Cs where extensibility effect on buckling loads is neglected.

C[a]							
K[a]	10^{-3}	10^{-2}	10^{-1}	1	10	10^2	∞[b]
P_{cr}[kN]							
10^{-10}	47.530231	80.054250	89.733663	90.848494	90.961533	90.972852	90.974109
10^{-5}	47.530906	80.056472	89.736485	90.851387	90.964432	90.975752	90.977010
10^{-3}	47.597385	80.275740	90.015088	91.137010	91.250768	91.262160	91.296999
10^{-2}	48.175702	82.211406	92.484455	93.669750	93.789955	93.801992	93.838765
10^{-1}	52.198430	97.230576	112.29400	114.06858	114.24940	114.26757	114.32178
1	60.990319	144.51524	184.41678	189.61832	190.15844	190.21392	190.36076
10^1	66.364695	197.22114	286.64986	298.74899	299.99518	300.12154	300.47186
10^2	67.554302	212.56628	323.36548	338.77443	340.41864	340.57747	341.04721
10^3	67.700260	214.52501	328.41593	344.39283	346.03217	346.19640	346.66198
10^5	67.717259	214.75489	329.01354	345.05240	346.69713	346.86229	347.32169
10^{10}	67.717432	214.75713	329.01962	345.05911	346.70390	346.86876	347.32847

[a] In kN/cm^2.
[b] P_{cr} calculated by Schnabl and Planinc (2011), where $d = 0$ and $\varepsilon_{cr} = 0$.

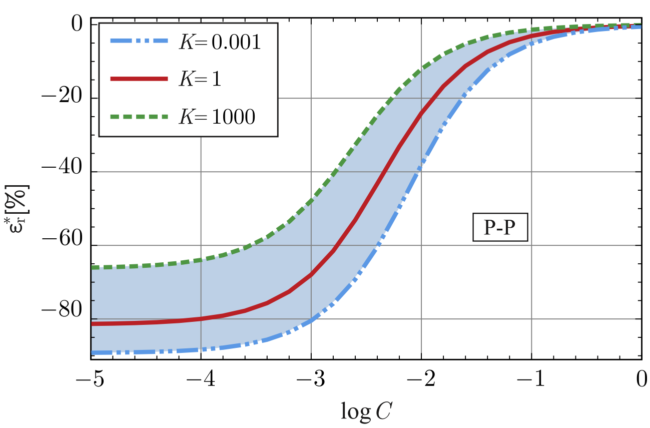

Fig. 4. The influence of interlayer uplift on critical buckling loads of P–P composite column for various Ks and Cs; where K, C are in [kN/cm^2].

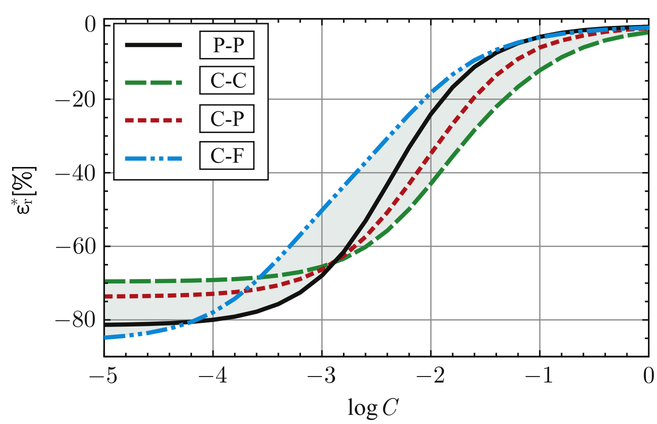

Fig. 5. The influence of interlayer uplift on critical buckling loads of composite column for different boundary conditions and various Cs and $K = 1$ kN/cm^2; C is also in [kN/cm^2].

Constraining equations:

$$\delta\Delta^* = \delta\Delta = \delta u^a - \delta u^b,$$
$$\delta d^* = \delta d = \delta w^a - \delta w^b,$$
$$\delta p_t^* = \delta p_t = K\delta\Delta,$$
$$\delta p_n^* = \delta p_n = C\delta d, \tag{18}$$

where

$$\varepsilon = \varepsilon^a = \varepsilon^b = -\frac{P}{C_{11}^a + C_{11}^b}, \quad \mathcal{N}^a = -\frac{C_{11}^a}{C_{11}^a + C_{11}^b}P,$$
$$\mathcal{N}^b = -\frac{C_{11}^a}{C_{11}^a + C_{11}^b}P, \tag{19}$$

and C denotes the linearized contact stiffness in transverse direction and d the uplift between the layers. All other variables have already been explained in detail by Schnabl and Planinc (2011).

Eqs. (15)–(19) constitute a system of 22 linear algebraic-differential equations of the first order with constant coefficients for 22 unknown functions: δu^a, δu^b, δw^a, δw^b, $\delta\varphi^a$, $\delta\varphi^b$, $\delta\varepsilon^a$, $\delta\varepsilon^b$, $\delta\gamma^a$, $\delta\gamma^b$, $\delta\kappa^a$, $\delta\kappa^b$, δR_X^a, δR_X^b, δR_Z^a, δR_Z^b, δM_Y^a, δM_Y^b, δp_t, δp_n, $\delta\Delta$, and δd along with the corresponding natural and essential boundary conditions written in the following general form as:

$x = 0$:

$$s_1^0\delta R_X^a(0) + s_2^0\delta u^a(0) = 0,$$
$$s_3^0\delta R_X^b(0) + s_4^0\delta u^b(0) = 0,$$
$$s_5^0\delta R_Z^a(0) + s_6^0\delta w^a(0) = 0,$$
$$s_7^0\delta R_Z^b(0) + s_8^0\delta w^b(0) = 0,$$
$$s_9^0\delta M_Y^a(0) + s_{10}^0\delta\varphi^a(0) = 0,$$
$$s_{11}^0\delta M_Y^b(0) + s_{12}^0\delta\varphi^b(0) = 0, \tag{20}$$

$x = L$:

$$s_1^L\delta R_X^a(L) + s_2^L\delta u^a(L) = 0,$$
$$s_3^L\delta R_X^b(L) + s_4^L\delta u^b(L) = 0,$$
$$s_5^L\delta R_Z^a(L) + s_6^L\delta w^a(L) = 0,$$
$$s_7^L\delta R_Z^b(L) + s_8^L\delta w^b(L) = 0,$$
$$s_9^L\delta M_Y^a(L) + s_{10}^L\delta\varphi^a(L) = 0,$$
$$s_{11}^L\delta M_Y^b(L) + s_{12}^L\delta\varphi^b(L) = 0, \tag{21}$$

where $s_i \in \{0, 1\}$ are the parameters that determine different combinations of boundary conditions of the two-layer composite column. The superscripts "0" and "L" of s identify its value at $x = 0$ and $x = L$, respectively.

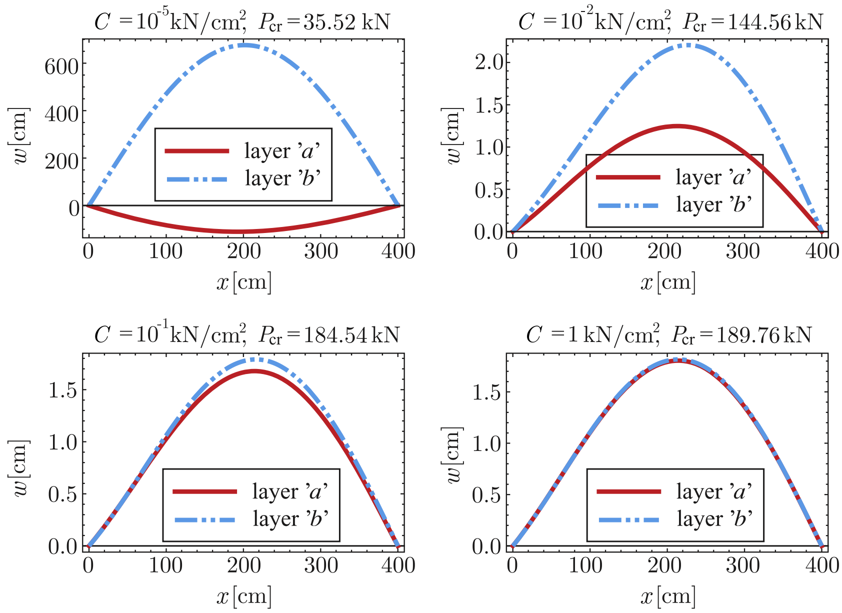

Fig. 6. The first buckling modes of layers *a* and *b*, and critical buckling loads of P–P composite column for $K = 1$ kN/cm^2 and various values of *C*; where *C* [kN/cm^2].

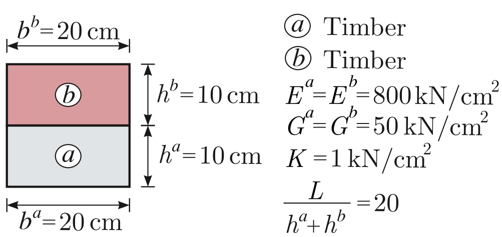

Fig. 7. Geometrical and material properties of timber-timber composite column.

2.2. Exact solution of the buckling problem

The system of linear algebraic-differential equations (15)–(19) and the corresponding natural and essential boundary conditions (20), (21) can be written as a homogeneous system of 12 first order linear differential equations as

$$\boldsymbol{Y}'(x) = \boldsymbol{A}\boldsymbol{Y}(x), \tag{22}$$

and

$$\boldsymbol{Y}(0) = \boldsymbol{Y}_0, \tag{23}$$

where $\boldsymbol{Y}(x)$ is the vector of unknown functions, $\boldsymbol{Y}(0)$ is the vector of unknown integration constants, and $\boldsymbol{A}$ is a constant real 12×12 matrix. The exact solution of the problem is given by, see e.g. (Perko, 2001):

$$\boldsymbol{Y}(x) = \exp^{\boldsymbol{A}x}\boldsymbol{Y}_0. \tag{24}$$

The unknown integration constants which are in this case the initial values of the generalized equilibrium internal forces and components of the displacement vectors, are determined from the boundary conditions (20) and (21). As a result, a system of 12 homogeneous linear algebraic equations for 12 unknown constants is obtained

$$\boldsymbol{K}\boldsymbol{Y}_0 = \boldsymbol{0}, \tag{25}$$

where $\boldsymbol{K}$ denotes the tangent stiffness matrix. A non-trivial solution of (25) is obtained from the condition of vanishing determinant of the matrix $\boldsymbol{K}$

$$\det \boldsymbol{K} = 0. \tag{26}$$

The condition (26) represents a linear eigenvalue problem. Its solution, i.e. the eigenvalues and eigenvectors correspond to the critical buckling loads, P_{cr}, and critical buckling modes of the column. An exact solution for the lowest buckling load, P_{cr}, and corresponding buckling mode can easily be determined but are generally too cumbersome to be presented as closed-form expressions.

3. Application, numerical results and discussion

The applicability of the proposed mathematical model for studying the buckling behaviour of geometrically perfect two-layer Reissner's composite columns with interlayer slip and uplift between the layers will be illustrated through the analysis of two numerical examples. The first example will be introduced to study the influence of interlayer uplift in combination with the interlayer slip on critical buckling loads and modes and to make a comparison of buckling loads calculated with and without taking uplift into account. In the second example, the effect of different boundary conditions of individual layers on its critical buckling loads and buckling modes will be analyzed. To this end, in both numerical examples, the critical buckling loads will be computed for a wide range of material and geometric parameters, such as interlayer slip modulus, *K*, interlayer uplift modulus, *C*, and different boundary conditions.

3.1. Effect of interlayer uplift on critical buckling loads and modes

In what follows, the effect of interlayer uplift in combination with the interlayer slip on critical buckling loads and modes is studied for a timber-concrete composite column analysed also by other researchers (see e.g., Girhammar and Pan, 2007; Schnabl and Planinc, 2010; and Xu and Wu, 2007). The geometrical and mechanical properties of this composite column are presented in Fig. 3.

The critical buckling loads are computed by the proposed mathematical model for various interlayer stiffnesses *K* and *C*, and different sets of boundary conditions summarized in Table 1.

The results for critical buckling loads in case of P–P composite column are presented in Table 2 for various interlayer stiffnesses

Table 4
Two combinations of the two-layer composite column boundary conditions.

Classical cases	C^a–F^a; F^b–C^b	P^a–P^a; F^b–C^b
Non-zero values	$s_2^0 = s_3^0 = s_6^0 = s_7^0 = s_{10}^0 = s_{11}^0 = 1$	$s_2^0 = s_3^0 = s_6^0 = s_7^0 = s_9^0 = s_{11}^0 = 1$
s_i	$s_1^L = s_4^L = s_5^L = s_8^L = s_9^L = s_{12}^L = 1$	$s_1^L = s_4^L = s_6^L = s_8^L = s_9^L = s_{12}^L = 1$
BCs scheme	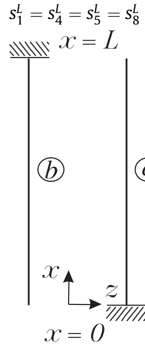	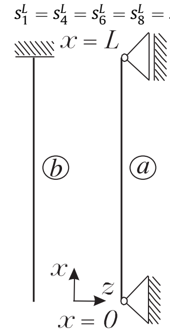

C = clamped (fixed); F = free; P = pinned; BC = boundary condition.

K and C. Evidently, the influence of the transverse interlayer stiffness, C, on critical buckling loads is significant and is dependent on K. Thus, the buckling loads decrease tremendously as K and C decrease. For example, the critical buckling load for almost freely sliding and uplifting composite column ($K = C = 0$) is approximately 7 times smaller compared to the buckling load of the same column but with an absolutely stiff connection between the two layers ($K = C = \infty; \Delta = d \to 0$). In addition, the influence of axial deformability on buckling loads is studied. The results are tabulated in Table 3. It can be seen that the axial deformability has a negligible influence on critical buckling loads of two-layer columns with interlayer slip and uplift.

Similarly, the effect of C is more pronounced for higher Ks. The dependence of this effect may be analysed by defining a relative error which is here defined as

$$\varepsilon_r^*[\%] = \frac{P_{cr}(\Delta \neq 0, d \neq 0) - P_{cr}(\Delta \neq 0, d = 0)}{P_{cr}(\Delta \neq 0, d \neq 0)} \times 100, \qquad (27)$$

where $P_{cr}(\Delta \neq 0, d \neq 0)$ and $P_{cr}(\Delta \neq 0, d \neq 0)$ are the critical forces obtained by the proposed exact procedure, where interlayer slip and uplift are taken into account, and by Schnabl and Planinc (2011) where interlayer uplift in neglected. The results for various interlayer slip moduli K and C are given in Fig. 4.

It is apparent from Fig. 4 that critical buckling loads decrease significantly if interlayer uplift is taken into account. For example, it is interesting to note that for a practical value of interlayer slip modulus $K = 1$ kN/cm^2, the corresponding relative errors are mostly considerable: $\varepsilon_r^*[\log C = -1] = -3.06\%$, $\varepsilon_r^*[\log C = -2] = -24.06\%$, $\varepsilon_r^*[\log C = -3] = -67.96\%$, $\varepsilon_r^*[\log C = -4] = -79.98\%$, $\varepsilon_r^*[\log C = -5] = -81.34\%$, while, in the two almost limiting cases, when there is nearly no connection between the layers ($\Delta \neq 0; K \approx 0$): $\varepsilon_r^*[\log C = -1] = -1.36\%$, $\varepsilon_r^*[\log C = -2] = -12.05\%$, $\varepsilon_r^*[\log C = -3] = -47.86\%$, $\varepsilon_r^*[\log C = -4] = -63.96\%$, $\varepsilon_r^*[\log C = -5] = -66.03\%$, or there is approximately an absolutely stiff connection between the layers ($\Delta \approx 0; K \approx \infty$), $\varepsilon_r^*[\log C = -1] = -5.16\%$, $\varepsilon_r^*[\log C = -2] = -38.11\%$, $\varepsilon_r^*[\log C = -3] = -80.47\%$, $\varepsilon_r^*[\log C = -4] = -88.35\%$, $\varepsilon_r^*[\log C = -5] = -89.19\%$. Evidently, this indicates that the effect of the uplift plays a very significant role in composite column buckling. The effect is negligible only for C smaller or approximately equal to 10^{-1} kN/cm^2. Furthermore, the influence of the uplift on critical buckling loads is investigated for different types of boundary conditions tabulated in Table 1. The results for $K = 1$ kN/cm^2 and various Cs are plotted in Fig. 5.

It is interesting to note that general distributions of the effect of the interlayer uplift on the critical buckling loads are rather similar for all types of boundary conditions. Nevertheless, this effect is for smaller Cs the greatest for C–C columns and the smallest for C–F columns, while, on the other hand, for higher Cs this effect is right the opposite.

At the end of this example, the first buckling modes of the individual layers a and b of the two-layer P–P composite column are calculated for $K = 1$ kN/cm^2 and various Cs. The results are given in Fig. 6. As would be expected, Fig. 6 shows that the layers a and b buckle almost independently for very small values of C, while for higher values the deformations of the layers become constrained. For example, when the layers are rather rigidly connected in the transverse direction, namely for $C \geqslant 1$ kN/cm^2, the first buckling modes of the two layers practically coincide.

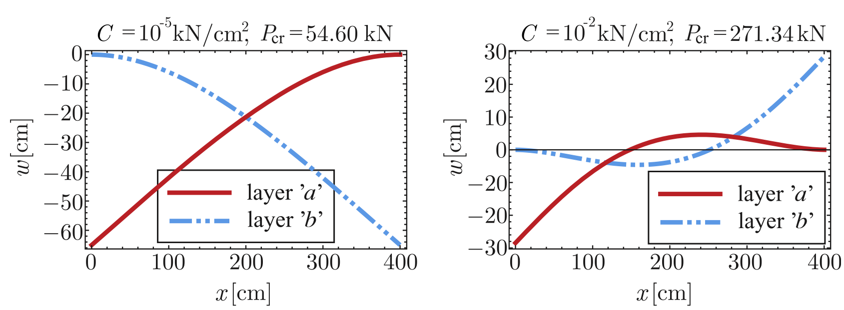

Fig. 8. Critical buckling loads and corresponding buckling modes for the first supporting combination for for $K = 1$ kN/cm^2 and various C; where C is in [kN/cm^2].

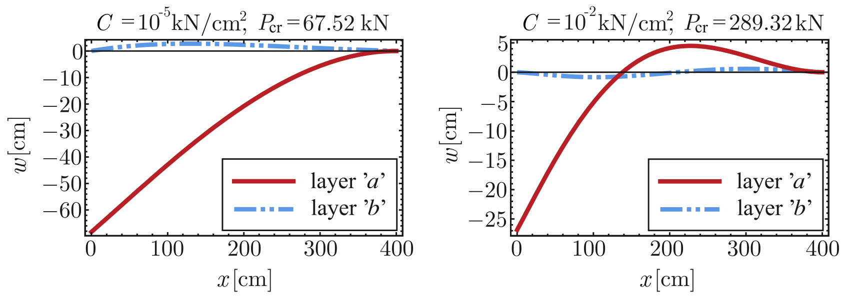

Fig. 9. Critical buckling loads and corresponding buckling modes for the second supporting combination for $K = 1$ kN/cm^2 and various C; where C is in [kN/cm^2].

3.2. Buckling modes and loads for different combinations of boundary conditions

The purpose of this numerical example is purely to demonstrate the capability of the proposed mathematical model to analyze different combinations of supporting conditions, i.e. different for each individual layer.

To this end, the critical buckling loads and the corresponding buckling modes are calculated for the two-layer composite column whose material and geometric parameters are given in Fig. 7 and considered boundary conditions summarized in Table 4.

The results for the first combination of boundary conditions (i.e. both layers are cantilever but supported at the opposite ends) are shown in Fig. 8 for $K = 1$ kN/cm^2 and various C (e.g. a realistic value for nailed connection with 10 nails per meter length is $C = 0.248$ kN/cm^2). It can be observed that layer's buckling modes are symmetrical compared to each other. Besides, it can be seen, that while the method in not constrained with the non-interpenetration condition, the layers can buckle over each other. Additionally, it can be seen that layers buckle freely for small Cs. On the other hand, the buckling modes are constrained for higher values of transverse interlayer stiffness, C. Thus, it is apparent that the interlayer uplift has a considerable influence not only on the critical buckling loads but also on the buckling modes of the layers.

Finally, the results for the second combination of boundary conditions are plotted in Fig. 9. Again, the effect of interlayer uplift, d, on critical buckling loads and corresponding buckling modes is negligible for small interlayer stiffness, C, while for higher values it is considerable should not be neglected.

4. Conclusions

The paper presented an efficient mathematical model for studying the buckling behaviour of geometrically perfect two-layer Reissner's composite columns with interlayer slip and uplift between the layers. The model is capable of predicting exact critical buckling loads and corresponding buckling modes. The effect of the transverse interlayer stiffness on the critical buckling loads were studied in detail. From the results obtained in the present study, the following conclusions can be drawn:

1. The effect of the transverse interlayer stiffness on the critical buckling loads is proved to be significant and interlayer slip modulus and boundary conditions dependent. Thus, the critical buckling loads obtained by the present analytical model can be up to approximately 89% smaller compared to those where interlayer uplift is neglected, i.e. for $C \approx \infty$.
2. As expected, it is observed that the critical buckling loads increases with the increasing of an interlayer uplift modulus, C.
3. The effect of the transverse interlayer stiffness on the buckling modes is proved to be considerable as well and can not be neglected for higher interlayer uplift stiffnesses.

References

Adekola, A., 1968. Partial interaction between elastically connected elements of a composite beam. Int. J. Solids Struct. 4 (11), 1125–1135.
Alfano, G., Crisfield, M.A., 2001. Finite element interface models for the delamination analysis of laminated composites: mechanical and computational issues. Int. J. Numer. Meth. Eng. 50, 1701–1736.
Amadio, C., Bedon, C., 2011. Buckling of Laminated Glass Elements in Compression. J. Struct. Eng. ASCE 137 (8), 803–810.
Challamel, N., Girhammar, U.A., 2011. Variationally-based theories for buckling of partial composite beam-columns including shear and axial effects. Eng. Struct. 33 (8), 2297–2319.
Challamel, N., Girhammar, U.A., 2012. Lateral-torsional buckling of vertically layered composite beams with interlayer slip under uniform moment. Eng. Struct. 34 (8), 505–513.
Chen, F., Qiao, P., 2011. Buckling of delaminated bi-layer beam-columns. Int. J. Solids Struct. 48 (18), 2485–2495.
Erkmen, R.E., Attard, M.M., 2011. Displacement-based finite element formulations for material-nonlinear analysis of composite beams and treatment of locking behaviour. Finite Elem. Anal. Des. 47 (12), 1293–1305.
Foraboschi, P., 2009. Analytical solution of two-layer beam taking into account nonlinear interlayer slip. J. Eng. Mech.-ASCE 135 (10), 1129–1146.
Gara, F., Ranzi, P., Leoni, G., 2006. Displacement-based formulations for composite beams with longitudinal slip and vertical uplift. Int. J. Numer. Meth. Eng. 65, 1197–1220.
Girhammar, U.A., Pan, D.H., 2007. Exact static analysis of partially composite beams and beam-columns. Int. J. Mech. Sci. 49 (2), 239–255.
Keller, H.B., 1970. Nonlinear bifurcation. J. Differ. Eqs. 7, 417–434.
Kim, S.H., Choi, J.H., 2011. Approximate analysis of simply supported composite beams with partial interaction. Adv. Struct. Eng. 14 (6), 1197–1204.
Kryžanowski, A., Schnabl, S., Turk, G., Planinc, I., 2009. Exact slip-buckling analysis of two-layer composite columns. Int. J. Solids Struct. 46, 2929–2938.
Kroflič, A., Planinc, I., Saje, M., Čas, B., 2010a. Analytical solution of two-layer beam including interlayer slip and uplift. Struct. Eng. Mech. 34 (6), 667–683.
Kroflič, A., Planinc, I., Saje, M., Turk, G., Čas, B., 2010b. Non-linear analysis of two-layer timber beams considering interlayer slip and uplift. Eng. Struct. 32, 1617–1630.
Kroflič, A., Saje, M., Planinc, I., 2011. Non-linear analysis of two-layer beams with interlayer slip and uplift. Comput. Struct. 89 (23–24), 2414–2424.
Le Grognec, P., Nguyen, Q.H., Hjiaj, M., 2012. Exact buckling solution for two-layer Timoshenko beams with interlayer slip. Int. J. Solids Struct. 49 (1), 143–150.
Nguyen, N.T., Oehlers, D.J., Bradford, M.A., 2001. An analytical model for reinforced concrete beams with bolted side plates accounting for longitudinal and transverse partial interaction. Int. J. Solids Struct. 38, 6985–6996.
Nguyen, Q.H., Hjiaj, M., Guezouli, S., 2011a. Exact finite element model for shear-deformable two-layer beams with discrete shear connection. Finite Elem. Anal. Des. 47 (7), 718–727.
Nguyen, Q.H., Martinelli, E., Hjiaj, M., 2011b. Derivation of the exact stiffness matrix for a two-layer Timoshenko beam element with partial interaction. Eng. Struct. 33 (2), 298–307.
Perko, L., 2001. Differential equations and dynamical systems, Third edition. Springer-Verlag, New York.
Ranzi, G., Ansourian, P., Gara, F., Leoni, G., Dezi, L., 2005. Displacement-based formulations for composite beams with longitudinal slip and vertical uplift. Department of Civil Engineering, The University of Sydney, Sydney, Australia. http://www.civil.usyd.edu.au.

Ranzi, G., Gara, F., Ansourian, P., 2006. General method of analysis for composite beams with longitudinal and transverse partial interaction. Comput. Struct. 84, 2373–2384.

Ranzi, G., Dall'Asta, A., Ragni, L., Zona, A., 2010. A geometric nonlinear model for composite beams with partial interaction. Eng. Struct. 32, 1384–1396.

Reissner, E., 1972. On one-dimensional finite-strain beam theory: The plane problem. J. Appl. Mech. Phys.-ZAMP 23, 795–804.

Robinson, H., Naraine, K.S., 1988. Slip and uplift effects in composite beams. In: International Conference on Composite Construction in Steel and Concrete. Proceedings of an Engineering Foundation Conference ASCE, Henniker, New Hampshire, pp. 487–497.

Schnabl, S., Saje, M., Turk, G., Planinc, I., 2007. Analytical solution of two-layer beam taking into account interlayer slip and shear deformation. J. Struct Eng.-ASCE 133 (6), 886–894.

Schnabl, S., Planinc, I., 2010. The influence of boundary conditions and axial deformability on buckling behavior of two-layer composite columns with interlayer slip. Eng. Struct. 32 (10), 3103–3111.

Schnabl, S., Planinc, I., 2011. The effect of transverse shear deformation on the buckling of two-layer composite columns with interlayer slip. Int. J. Nonlinear Mech. 46 (3), 543–553.

Volokh, K.Yu., Needleman, A., 2002. Buckling of sandwich beams with compliant interfaces. Comput. Struct. 80, 1329–1335.

Wells, G.N., De Borst, R., Sluys, L., 2002. A consistent geometrically non-linear approach for delamination. Int. J. Numer. Meth. Eng. 54, 1333–1355.

Xu, R., Wu, Y., 2007. Two-dimensional analytical solutions of simply supported composite beams with interlayer slips. Int. J. Solids Struct. 44, 165–175.